Heliyon 10 (2024) e34646

Contents lists available at ScienceDirect

Heliyon

journal homepage: www.cell.com/heliyon

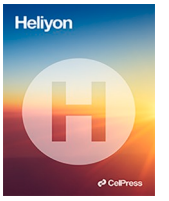

Research article

Layer-specific biomechanical and histological properties of normal and dissected human ascending aortas

Xiaoya Guo [a], Han Yu [b], Liang Wang [c,**], Yali Zhai [d], Jiantao Li [d,***], Dalin Tang [c,e], Haoliang Sun [f,*]

[a] School of Science, Nanjing University of Posts and Telecommunications, Nanjing, 210023, China
[b] School of Mechanical, Medical and Process Engineering, Queensland University of Technology, Brisbane, 4000, Australia
[c] School of Biological Science and Medical Engineering, Southeast University, Nanjing, 211189, China
[d] Department of Pathophysiology, Nanjing Medical University, Nanjing, 211166, China
[e] Mathematical Sciences Department, Worcester Polytechnic Institute, Worcester, MA, 01609, USA
[f] Department of Cardiovascular Surgery, First Affiliated Hospital of Nanjing Medical University, Nanjing, 210029, China

ARTICLE INFO

Keywords:
Aortic dissection
Biaxial tensile testing
Mechanical properties
Histological analysis
Constitutive modeling

ABSTRACT

Recent studies have attempted to characterize the layer-specific mechanical and microstructural properties of the aortic tissues in either normal or pathological state to understand its structural-mechanical property relationships. However, layer-specific tissue mechanics and compositions of normal and dissected ascending aortas have not been thoroughly compared with a statistical conclusion obtained. Eighteen ascending aortic specimens were harvested from 13 patients with type A aortic dissection and 5 donors without aortic diseases, with each specimen further excised to obtain three tissue samples including an intact wall, an intima-media layer and an adventitia layer. For each tissue sample, biaxial tensile testing was performed to obtain the experimental stress-stretch ratio data, which were further fed into the Fung-type model to quantify the tissue stiffness, and Elastin Van Gieson stain and Masson's trichrome stain were employed to quantify the elastic and collagen fiber densities. Statistical analyses were performed to determine whether any significant differences exist in mechanical properties and compositions between diseased and normal aortic tissues. The tissue stiffness of intima-media samples was significant higher in diseased group than that of normal group in longitudinal direction at the stretch ratio 1.30 ($p = 0.0068$), while no significant differences were found in the other direction or other tissue types. Even though there was no significant difference in elastic or collagen fiber densities between two groups, the diseased group generally had lower elastic fiber density, but higher collagen fiber density for all three tissue layers. Compared to normal aortic tissues, the elastic fiber density of the intima-media layer in the dissected aortic tissue was lower, while its tissue stiffness was significantly higher, indicating the tissue stiffness of the intima-media layer could be a potential indicator for aortic dissection.

* Corresponding author.
** Corresponding author.
*** Corresponding author.
E-mail addresses: liangwang@seu.edu.cn (L. Wang), ljt@njmu.edu.cn (J. Li), shlsky@126.com (H. Sun).

https://doi.org/10.1016/j.heliyon.2024.e34646
Received 3 March 2024; Received in revised form 22 June 2024; Accepted 12 July 2024
Available online 14 July 2024

1. Introduction

Aortic dissection (AD) is a life-threatening condition with an overall in-hospital mortality rate of 27.4 % for the patients in the acute

Abbreviation list

AD	aortic dissection
Adv	adventitia layer
BP	blood pressure
EC	incremental elastic moduli in circumferential direction
EL	incremental elastic moduli in longitudinal direction
IM	intima-media layer
IW	intact wall
EVG	Elastin Van Gieson

phase [1–3]. AD is characterized by the intimal tear progressing into the aortic media, which would form a blood filled cavity or channel within the aortic wall [4,5], and could cause devastating sequelae, such as aortic rupture, acute severe aortic regurgitation, and malperfusion causing end-organ ischemia or infarction if left untreated [6]. The intimal tear starts when the hemodynamic loading and wall mechanics break the presumably already weakened aortic wall resulting from pathological tissue remodeling [7,8]. Thus, it is of pressing need to study the mechanical and microstructural alterations in the aortic tissue to have a deeper understanding of the underlying mechanism developing this disease [9,10].

The weakening of the aortic wall stems from the changes in its microstructural properties, including elastin and collagen fiber contents, fiber organizations and their cross-linking [11,12]. During the pathological development of various aortic diseases, the aortic wall undergoes both extracellular matrix remodeling and mechanical properties alteration simultaneously [11,13,14]. Efforts have been exerted to investigate the impact of aortic diseases on the detailed mechanical and microstructural properties of the aortic tissues via biaxial tensile testing and histological analysis [15–19]. But most previous studies focused on comparing the aneurysmal and normal ascending thoracic aortic tissues for aortic aneurysm rupture risk stratification [20]. In a 41 patients study, Nightingale et al. claimed that the decreased elastin content in the aortic tissue may be response for low tissue elastic modulus at low strain level [21]. A more detailed layer-specific investigation revealed that, compared to the normal aortic tissue, aneurysmal aortic tissues were stiffer, and had less elastic fiber content, but no significant differences in the tissue strength and the collagen fiber content were found between two types of tissues [13]. Layer-specific mechanical and microstructural properties of the human aortic tissue were also investigated [22,23]. Amabili et al. studied microstructural and mechanical characterization of tissue layers of healthy descending aorta using second harmonic generation, two-photon fluorescence images and uniaxial tensile tests [24]. Pukaluk et al. investigated the microstructural changes of the human atherosclerotic abdominal aortic media under biaxial loading using multi-photon microscopy. Their observations in microstructural alterations could provide an explanation of the exhibited mechanical behavior of the aortic media [18]. Similar approach was applied to illustrate the structural-mechanical relationship of the human aortic adventitia [19]. Despite rapid progress were made, a comparison analysis of the layer-specific aortic tissue mechanics and histology between dissected and normal aortas would still advance our understanding of the development of aortic dissection.

Here, we attempt to quantify and compare the mechanical behavior and histological characteristics of the diseased aortic specimens from patients with Type A AD and normal aortic specimens from donors. Biaxial tensile testing was performed to characterize the layer-specific mechanical properties of both normal and diseased aortic tissues. Quantitative histological analysis was carried out to quantify the elastic and collagen fiber densities in the tissue samples. Statistical analysis was performed to compare the difference in mechanical and histological properties in two tissue groups to determine if mechanical and histological anomalies are associated with the disease.

2. Materials and methods

2.1. Aortic tissue preparation

Ascending aortic tissue specimens were harvested from patients with type A aortic dissection (diseased group, n = 13) and organ donors without aortic diseases (normal group, n = 5) at Jiangsu Province Hospital with informed consents obtained. One diseased aortic specimen was obtained from each patient who underwent surgical repair of aorta following Sun's procedure [25]. For comparison purpose, five normal aortic specimens were also collected from five donors as the control group. The cause of death of five donors are traumatic brain herniation (n = 2), severe traumatic brain injury (n = 2) and spontaneous intracerebral hemorrhage (n = 1). All specimens were acquired from the ascending aortic segment about 1–5 cm above the sinotubular junction. Clinical information, including age, gender among others were acquired following the protocol approved by the Medical Ethics Committee of Jiangsu Province Hospital (approval number: 2022-SR-730).

All tissue specimens were preserved in a cryopreservation agent in a −80 °C freezer prior to the mechanical testing and histological

analysis. The cryopreservation agent composed of 85 % culture medium (RPMU 1640), 5 % albumin solution (20 %), and 10 % dimethyl sulfoxide was utilized to prevent tissue damage due to freezing [26,27]. To investigate what kind of mechanical and histological alterations make the aortic wall predispose to the consequent fatal AD event, the non-dissected site adjacent to dissection flap was selected as the pre-dissection state of the dissected aortic specimen, to perform direct comparison with the normal aorta. To that end, two square samples with dimensions about 20 × 20 mm were cut out from the non-dissected sites for each tissue specimen after thawing. One square sample was separated into intima-media layer (IM) and adventitia layer (Adv) since the tear typically develops into both intima and media layers together in aortic dissection (Fig. 1(b)), while the other sample was kept as intact wall (IW) with full three layers [22,28]. In total, 54 tissue samples in three sample types (one IW, IM and Adv sample from each aortic specimen) from both normal and diseased groups were prepared and subjected to subsequent biaxial tensile testing. Sample thickness was measured by averaging the thickness values at four different locations using a digital caliper (Mitutoyo 500-197-30, resolution: 0.01 mm). Fig. 1 shows schematic illustration of the specimen preparation, experimental testing and histological analysis.

2.2. Biaxial tensile testing and constitutive modeling

For all 54 tissue samples, each sample was mounted into a biaxial testing system (IPBF-300, CARE Measurement & Control) using fisher hook clamps [29,30], while immersed in the phosphate-buffered saline with the temperature controlled at around 37 °C (Fig. 1 (c)) [31]. Biaxial tensile testing was performed in a force-driven manner following a previously established procedure [30]. Briefly speaking, after 10 preconditioning cycles to reduce tissue hysteresis, five consecutive protocols with the following force ratios in circumferential and longitudinal directions: 1:1, 1:0.75, 0.75:1, 1:0.5, and 0.5:1 with the maximal force of 2.0 N were applied to the sample, and the forces and displacements of all samples in two directions were recorded continuously to calculate the stress-stretch

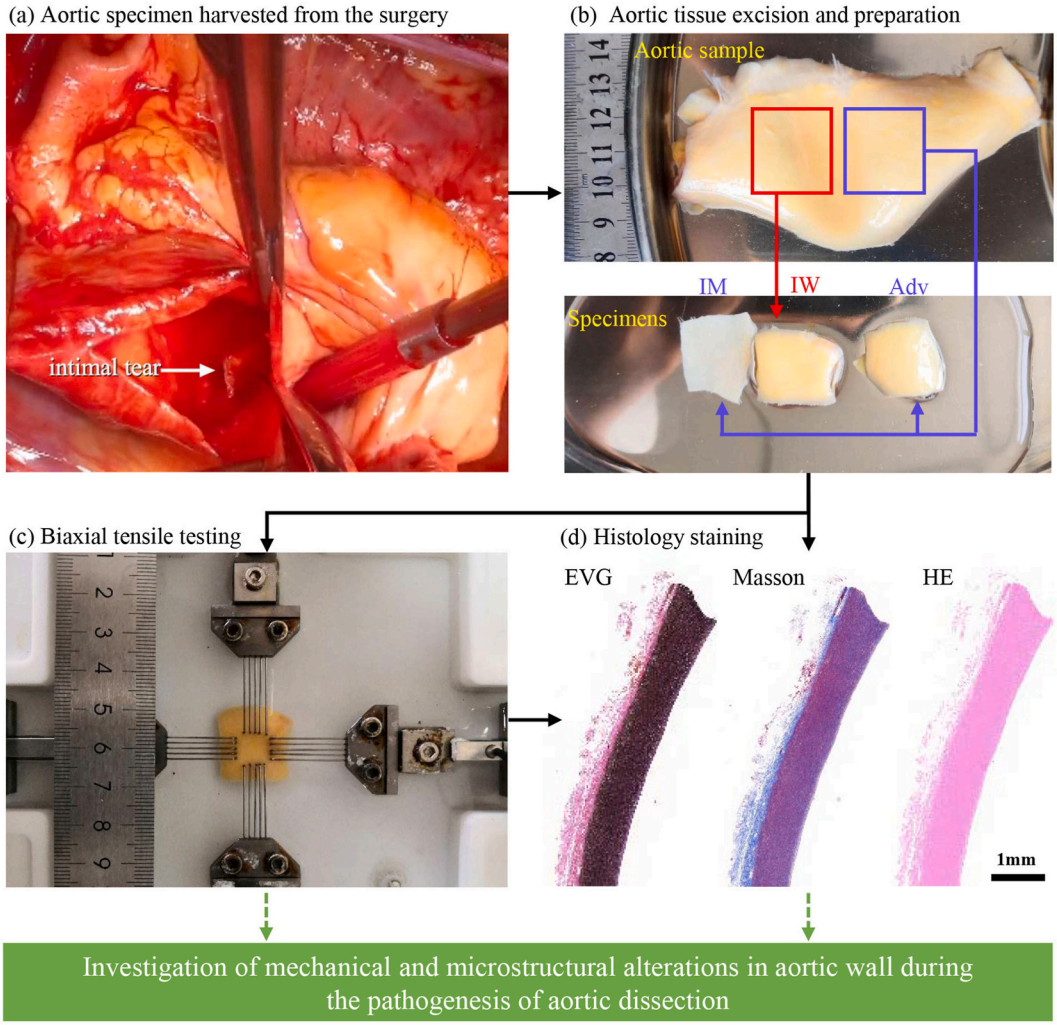

Fig. 1. Schematic illustration of the specimen harvesting, preparation and experimental analyses. (a) Aortic specimen harvested from the surgery; (b) Aortic tissue excision and preparation; (c) Biaxial tensile testing; (d) Histological staining.

ratio (σ–λ) data [32–34]. Since the calculation of stress-stretch ratio data were sensitive to the preloading force, especially for Adv samples, the tissue configuration under 0.01 N pre-load was defined as the initial zero-stretch state [35].

All aortic tissues were assumed to be an incompressible homogeneous and hyperelastic material. Fung-type material model was used to fit the stress-stretch ratio data with the following strain energy density function [15,27]:

$$W = \frac{C}{2}(\exp(Q) - 1) \tag{1}$$

where $Q = c_1E_c^2 + 2c_2E_cE_z + c_3E_z^2$, E_c and E_z are the circumferential and longitudinal Green-Lagrange strain values, which could be derived from stretch ratio data, and C, c_1, c_2, c_3 are material parameters. Trust-region-reflective algorithm was employed to determine the material parameters, and the coefficient of determination (R^2 value) was calculated to measure the goodness-of-fit [27,35]. More information on the derivation for data fitting were provided in the Supplementary File (Section A).

2.3. Quantitative histological analysis

After mechanical testing, histological staining was performed to visualize the aortic tissue components of three samples (IW, IM and Adv tissue samples) for a subset of subjects (n = 7 from diseased group, and n = 5 from normal group) following the established procedure [13,36]. A subsample was excised from each tested sample and fixed in formalin for 24 h, and then dehydrated through a process of varied alcohol concentrations, embedded in paraffin, and serially sectioned into a 5-μm thickness section [13,23]. Consecutive sections were stained with Elastin van Gieson (EVG) for elastic fiber, Masson's trichrome for collagen fiber, and hematoxylin–eosin for gross aortic wall morphology, respectively [13,14,23]. The histological staining of all samples were done in one batch to minimize any batch effects due to intra-operator or inter-operator variability. All histological slides were imaged with digital slide

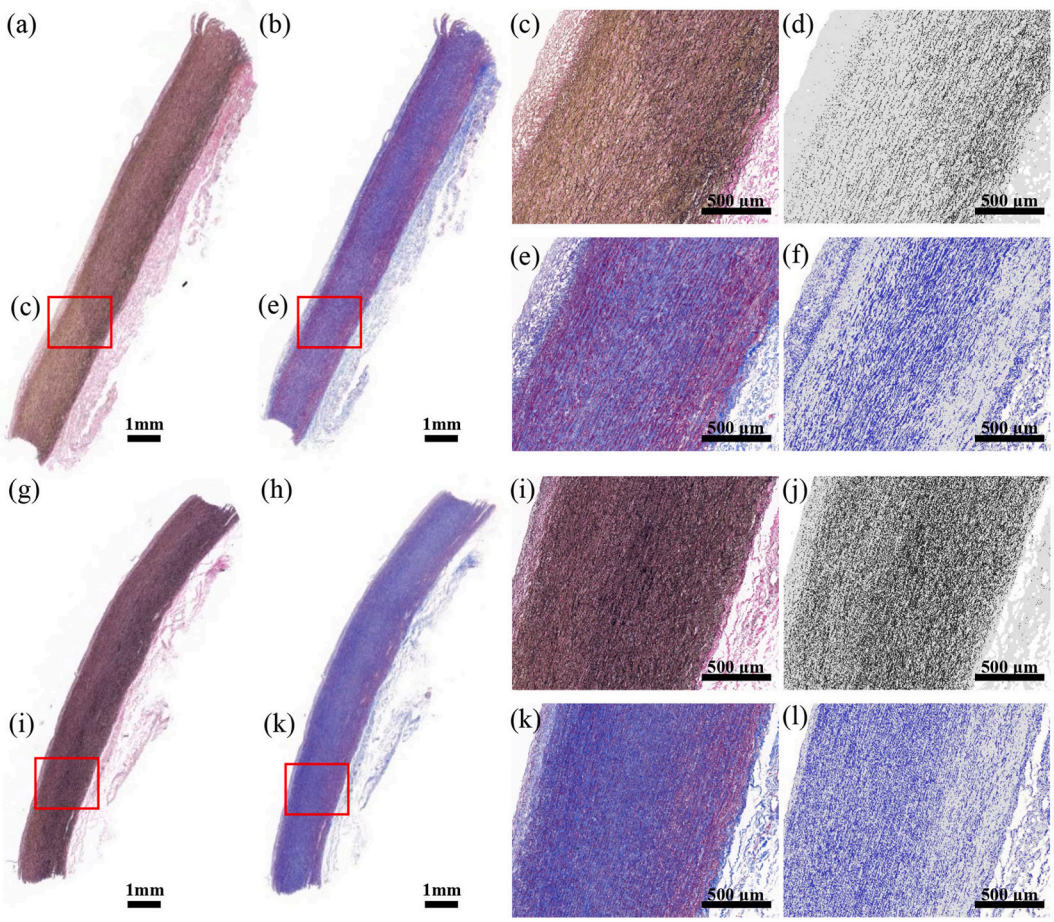

Fig. 2. Representative images of EVG and Masson staining of diseased (a–b) and normal (g–h) aortic IW samples. (c–d) Enlarged views of EVG staining image at a sample site of diseased IW sample, and its segmentation for elastic fiber content; (e–f) Enlarged views of Masson staining image at the same sample site of diseased aortic specimen, and its segmentation for collagen fiber content; (i–l) Enlarged views of EVG staining and Masson staining images at a sample site of normal IW sample, and the segmentation for elastic and collagen fiber contents, respectively.

scanner (Pannoramic MIDI, 3DHISTECH) to extract the elastic and collagen fibers components using the threshold value algorithm from EVG images and Masson images, respectively (Fig. 2) [26,37]. After deleting the background region, the areal percent occupied by each stained fiber over the entire tissue sample was calculated to define the fiber density [13,37]. Fig. 2 shows the image processing of the EVG and Masson images of one diseased and one normal IW sample.

2.4. Statistical analysis

Due to the small sample size of aortic specimens, the results obtained for diseased group and normal group do not satisfy the normality assumption after checking with Shapiro-Wilk test [38]. Nonparametric Mann-Whitney *U* test was used to determine whether any significant differences in material properties and aortic tissue components exist between two groups for three sample types [39]. Statistical analysis was performed with MATLAB (MathWorks) with a statistical significance level of 0.05.

3. Results

3.1. Subject characteristics and sample information

The subject characteristics and tissue sample information of all 18 patients/donors are listed in Table 1, including clinical information, sample thickness of three sample types, and indication for histological stain. The sample thickness of three sample types from the diseased group were all thicker than those from the normal group. However, only the differences in IW and Adv samples thickness were statistically different ($p = 0.0425$ and $p = 0.0135$, respectively).

3.2. Constitutive modeling of diseased and normal aortic tissues

Experimental stress-stretch ratio data from biaxial tensile testing were used to fit the Fung-type model to determine the material parameters for all 54 tissue samples. Representative material curves from diseased and normal groups were shown in Fig. 3. All tissue samples exhibited a J-shape material curves indicating the nonlinear stress-stretch behavior with increased tissue stiffness when stretched. The summary of the material parameters for each sample type is provided in Table 2, while more details on material parameters for each sample are given in Supplementary File (Table S1). The average R^2 value for all 54 samples is 0.9634, indicating that the Fung-type model can accurately describe the mechanical behaviors of different layers of the aortic tissue.

3.3. Tissue stiffness difference between diseased and normal tissue samples

Considering the nonlinearity of the material curves, the incremental elastic modulus defined as the slope of tangent line to the stress-stretch curve at given stretch ratio was used to measure the tissue stiffness using the following formula: $E(\lambda) = d\sigma/d\lambda$, where E is the incremental elastic modulus [40]. Table 3 summarizes the incremental elastic moduli in both circumferential and longitudinal directions (denoted as EC and EL, respectively) at the stretch ratio interval [1.0, 1.4] for all tissue samples. As expected, the tissue stiffness elevated at higher stretch ratio. An interesting observation was that the tissue stiffness of diseased tissue samples increased faster than normal tissue samples, as can been seen in IW samples in longitudinal direction, IM and Adv samples in circumferential direction. This is consistent with the observation in material curves that diseased tissues tended to start with lower stress response at low stretch ratio level and increase faster than normal tissues (see Fig. 3).

Table 1
Clinical characteristics and tissue sample information of all 18 subjects. Abbreviation: BP, blood pressure; D, diseased group; N, normal group; IW, intact wall; IM, intima-media layer; Adv, adventitia layer.

Subject ID	Gender	Age	Height (cm)	Weight (kg)	BP (mmHg)	IW thickness (mm)	IM thickness (mm)	Adv thickness (mm)	Histology
D1	Male	51	168	84.5	168/59	1.50	1.25	0.50	No
D2	Male	48	176	100	139/71	2.42	1.46	0.70	No
D3	Male	49	172	60	126/65	2.21	1.66	0.66	No
D4	Male	58	170	80	139/63	1.75	1.34	0.54	No
D5	Male	41	178	70	99/57	1.68	1.29	0.58	No
D6	Male	49	175	95	124/73	1.74	1.22	0.49	No
D7	Male	61	177	78	145/71	2.51	2.08	0.67	Yes
D8	Female	58	162	57.5	141/99	2.80	1.97	0.60	Yes
D9	Male	51	170	80	148/63	1.29	1.21	0.54	Yes
D10	Male	46	165	67	131/80	1.58	1.17	0.60	Yes
D11	Male	55	170	70	163/70	1.29	1.16	0.40	Yes
D12	Female	53	168	85	177/81	1.42	0.97	0.39	Yes
D13	Male	45	176	100	109/62	1.70	0.91	0.43	Yes
N1	Male	37	170	83	117/75	1.66	1.37	0.52	Yes
N2	Male	32	170	60	133/80	1.33	1.22	0.27	Yes
N3	Male	42	175	75	124/83	1.31	1.15	0.18	Yes
N4	Female	45	160	65	140/74	1.44	0.91	0.48	Yes
N5	Male	54	175	70	113/75	1.20	0.91	0.25	Yes

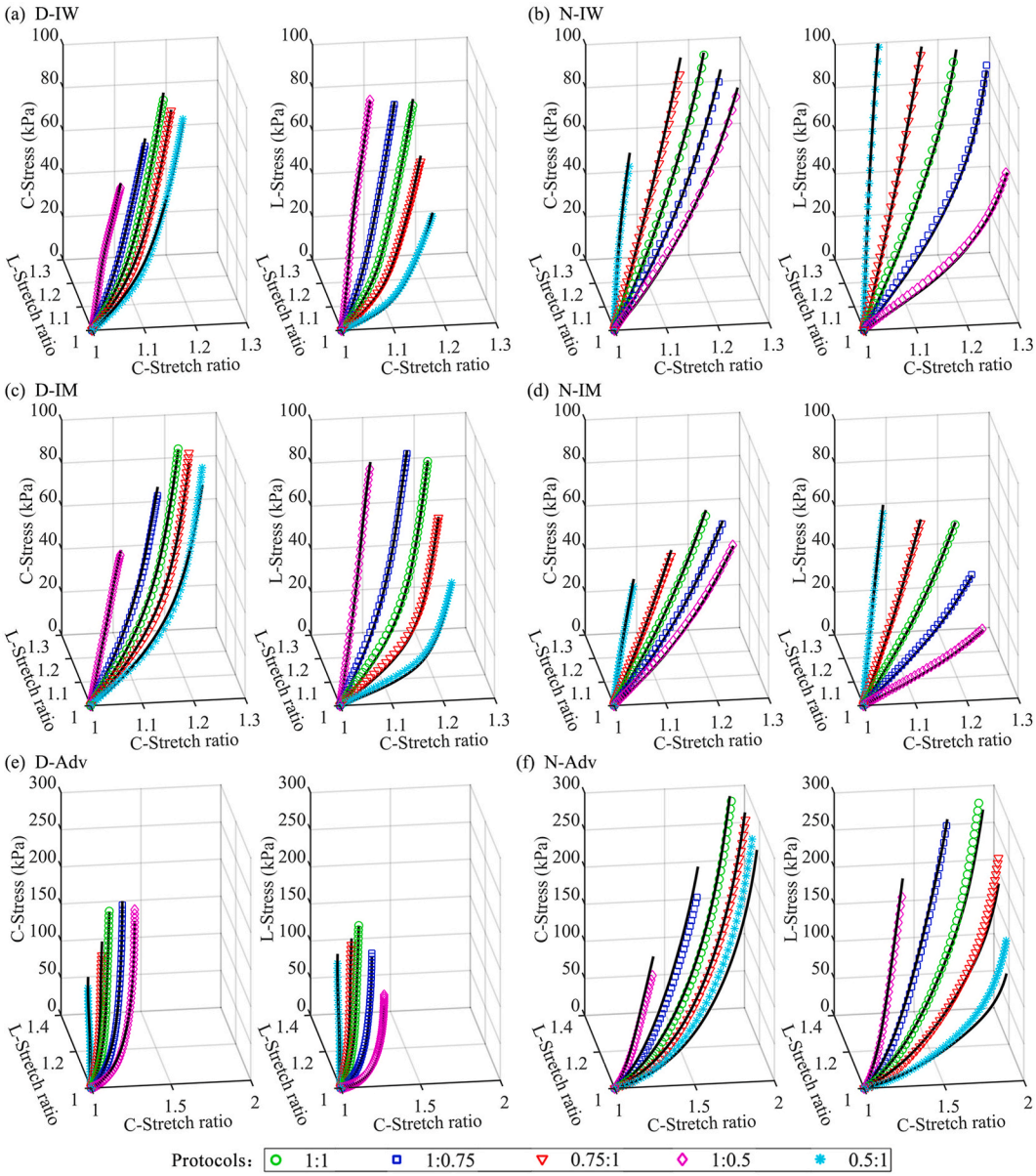

Fig. 3. Representative biaxial mechanical stress-stretch ratio data and fitted material curves of three sample types from a sample patient (D7) and a sample donor (N5). Material curves in circumferential and longitudinal directions of intact wall (a), intima-media layer (c), and adventitia layer (e) from a sample patient; intact wall (b), intima-media layer (d), and adventitia layer (f) from a sample donor. Different protocol was indicated by the color at the bottom. (For interpretation of the references to color in this figure legend, the reader is referred to the Web version of this article.)

Table 2
Summary of material parameters for three sample types from diseased and normal groups. Values are median (25th, 75th percentiles). Abbreviation: D, diseased group; N, normal group; IW, intact wall; IM, intima-media layer; Adv, adventitia layer.

Sample type	C (kPa)	c_1	c_2	c_3	R^2
D-IW	155.5 (52.4, 267.4)	0.77 (0.47, 2.61)	0.22 (0.13, 0.27)	0.62 (0.44, 1.96)	0.9953 (0.9867, 0.9975)
N-IW	438.0 (147.8, 1592.9)	0.44 (0.08, 0.86)	0.14 (0.03, 0.27)	0.35 (0.07, 0.84)	0.9962 (0.9958, 0.9975)
D-IM	206.7 (49.4, 990.1)	0.49 (0.11, 2.47)	0.17 (0.05, 0.36)	0.55 (0.13, 1.75)	0.9960 (0.9673, 0.9984)
N-IM	616.9 (472.1, 1203.5)	0.18 (0.13, 0.30)	0.06 (0.05, 0.10)	0.14 (0.12, 0.23)	0.9982 (0.9937, 0.9984)
D-Adv	42.6 (26.7, 82.5)	2.57 (1.30, 2.98)	0.37 (0.17, 0.65)	2.06 (1.68, 3.68)	0.9488 (0.9061, 0.9854)
N-Adv	301.1 (151.5, 331.2)	0.59 (0.51, 0.84)	0.18 (0.11, 0.23)	0.81 (0.53, 0.97)	0.8515 (0.8412, 0.9165)

Table 3
Summary of tissue stiffness in both circumferential and longitudinal directions at different stretch ratio for three sample types from diseased and normal groups. Values are median (25th, 75th percentiles). Abbreviation: D, diseased group; N, normal group; IW, intact wall; IM, intima-media layer; Adv, adventitia layer. Unit of EC and EL: kPa.

Sample type		$\lambda = 1.0$	$\lambda = 1.1$	$\lambda = 1.2$	$\lambda = 1.3$	$\lambda = 1.4$
D-IW	EC	119.9 (109.8, 131.8)	191.1 (177.9, 212.1)	294.1 (281.6, 338.3)	467.3 (414.6, 638.1)	734.7 (672.1, 1341.7)
	EL	111.8 (82.4, 120.3)	182.9 (133.8, 190.3)	275.6 (248.2, 299.1)	414.9 (391.6, 474.2)	647.5 (594.4, 989.8)
N-IW	EC	117.2 (114.2, 138.7)	188.6 (181.8, 218.8)	287.1 (266.5, 347.7)	439.1 (370.2, 563.3)	681.0 (499.0, 951.9)
	EL	115.5 (99.0, 133.9)	180.7 (156.9, 216.5)	263.0 (237.3, 347.7)	390.5 (334.9, 545.3)	597 (451.0, 841.4)
D-IM	EC	110.2 (82.9, 123.8)	173.6 (139.6, 208.6)	264.9 (249.2, 320.5)	449.3 (356.4, 555.3)	609.8 (511.8, 1330.6)
	EL	105.1 (87.5, 134.1)	164.7 (145.4, 210.6)	261.7 (232.4, 307.4)	408.4 (380.8, 465.0)	616.9 (588.0, 743.8)
N-IM	EC	121.1 (107.9, 145.7)	192.1 (169.3, 228.1)	292.0 (248.4, 332.2)	437.7 (350.7, 462.6)	600.5 (484.1, 670.2)
	EL	103.7 (86.3, 119.2)	164.2 (135.3, 186.8)	247.7 (197.9, 272.7)	360.7 (277.8, 386.0)	494.6 (380.2, 555.7)
D-Adv	EC	76.6 (49.0, 162.2)	133.4 (80.6, 261.6)	263.7 (138.4, 438.5)	551.4 (230.0, 792.8)	1026.8 (432.7, 1749.8)
	EL	94.5 (65.9, 131.5)	156.8 (111.0, 214.6)	271.4 (200.6, 381.6)	503.4 (367.7, 834.5)	1015.6 (721.3, 1796.0)
N-Adv	EC	177.0 (63.8, 307.3)	281.2 (100.8, 492.2)	428.3 (151.4, 768.5)	644.7 (222.3, 1206.7)	977.2 (325.3, 1943.3)
	EL	194.7 (76.9, 249.0)	309.6 (121.5, 402.1)	473.0 (185.2, 643.5)	715.9 (282.7, 1052.5)	1093.5 (438.0, 1793.9)

Statistical analysis was performed to test whether significant difference in tissue stiffness exists between diseased and normal groups at stretch level 1.3 (Fig. 4), given that human aorta typically work at this stretch level under the physiological conditions [41]. Mann-Whitney *U* test showed that EL of the IM samples from the diseased group was significantly higher than that from the normal group ($p = 0.0068$) while no significant difference was found in the other direction or other sample types. Numerically speaking, IW and IM samples from the diseased group generally were stiffer than those from the normal group, while Adv samples were overall softer in the diseased group.

3.4. Comparison in histological properties between diseased and normal tissue samples

As can be seen in Fig. 2, the elastic fiber structure in the aortic media from the diseased group was disorganized and thinner, compared to the IM sample from the normal group. More quantitative analysis on the elastic and collagen fiber densities in three sample types of both groups are shown in Fig. 5. By gross observation, tissue samples from the diseased group had lower elastic fiber density, but higher collagen fiber density, compared to those from the normal group. Based on the analyzed aortic samples, no statistical difference in both elastic and collagen fiber densities was found between the diseased and normal groups for any sample type. Numerically, the median values of elastic fiber density in IW, IM and Adv samples from diseased group were 21.4 %, 22.2 %, and 40.5 % less than those from normal group. Compared to the elastic fiber density, the two groups generally were close in collagen fiber density, with the relative difference less than 8.5 %.

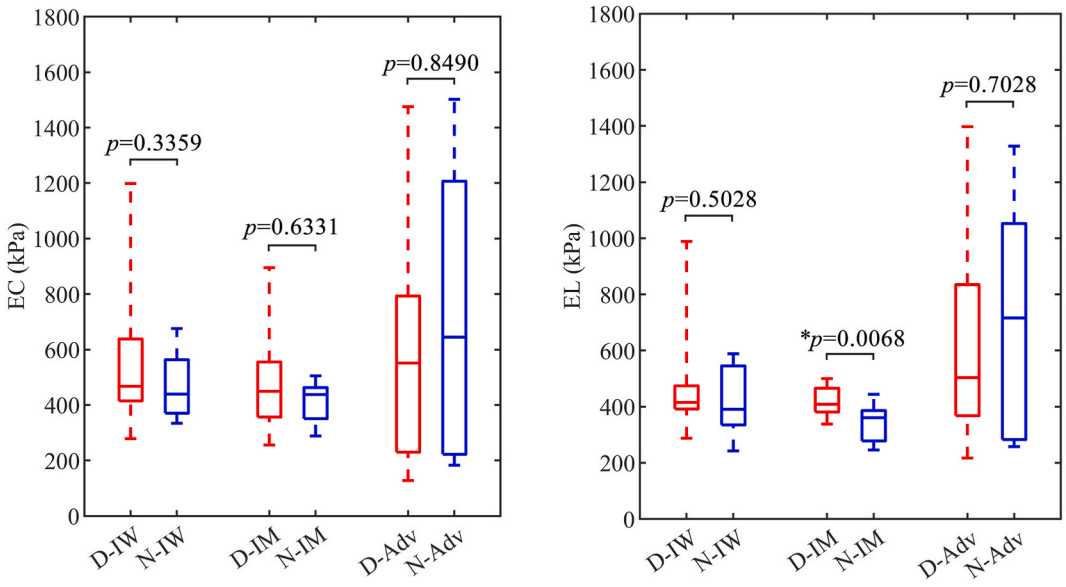

Fig. 4. Comparison in tissue stiffness of three sample types between diseased and normal groups.

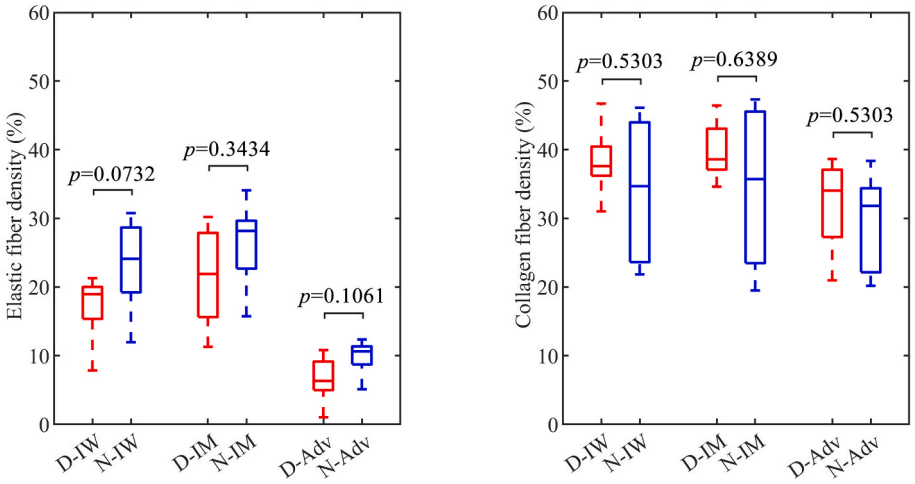

Fig. 5. Comparison in elastic and collagen fiber densities of three sample types between diseased and normal groups.

4. Discussion

The pathological mechanisms to aortic dissection are not fully understood [7,42,43]. It is of great importance to investigate the mechanical and histological changes in the aortic wall at the pre-dissection stage, so that a better understanding why aortic dissection would eventually happen to these diseased aortas could be gained. Clinical observations have showed that pre-dissected aorta normally undergoes extracellular matrix remodeling, leading to the weakened wall prone to dissection [6,44]. Recent literature showed that the experimental analysis combining mechanical testing and histological staining was the powerful method for exploring aortic diseases, which is beneficial to understand the mechanical and histological alterations in the aortic tissue during disease progression [18,19,22–24]. This study was intended to simultaneously quantify the changes in both biomechanical and histological properties of the normal and dissected ascending aortic wall, and its structural-functional relationship to identify potential indicator for dissection risk assessment [9,11,14].

Even though there are other classical material models, such as modified anisotropic Mooney-Rivlin model [30], Holzapfel-Gasser-Ogden model [45] and four-fiber family constitutive models [46,47] among others, to describe the mechanical properties of aortic tissue, Fung-type model is also widely used and was chosen as the constitutive model in this study [15]. This model is simple and can accurately capture the mechanical properties of the normal and diseased aortic tissues. The average R^2 value for all 54 samples is 0.9634, indicating its good fitting performance. In fact, in our preliminary test, we tried to perform the data fitting using both Fung-type and modified anisotropic Mooney-Rivlin model to compare their fitting performance. The result (data not reported) showed that the fitting performance of both models are very close. Fig. 3 shows Fung-type model-based fitted material curves of three sample types from a sample patient (D7) and a sample donor (N5) using five consecutive protocols. Fig. 3 and Table 3 illustrate the nonlinearity of tissue mechanical properties, and also display that material stiffness of diseased tissue samples in circumferential and longitudinal directions increased faster than that of normal tissue samples when stretch ratio increased from 1.1 to 1.4.

4.1. Changes in mechanical properties during aortic dissection

Few studies exist to compare the mechanical properties between diseased tissues with aortic dissection and normal aortic tissues [14,23]. Previous studies were more focus on the impact of ascending aortic aneurysm on aorta mechanics [48]. However, some inconsistency exists in the current literature, regarding whether aneurysmal tissue is significant stiffer than normal tissue in the ascending aorta [9,49,50]. Most studies reported that aneurysmal aortic tissues had higher tissue stiffness than normal tissues [50,51]. Using uniaxial testing, Vorp et al. claimed that aortic aneurysmal tissues were significantly stiffer in longitudinal direction, but not significantly stiffer in circumferential direction [48]. On the contrary, Azadani et al. found that no significant difference in tissue stiffness was found in both directions between aneurysmal and normal aortic tissues based on 37 specimens [49]. More surprisingly, another study reported that at low strain level, normal tissue was stiffer [9].

The inconsistency in the current literature could be unified by a theory proposed recently [21]. Due to the nonlinearity of tissue mechanical properties, aortic stiffness changes with respect to different strain or stretch levels. Thus the conclusion of whether aneurysmal tissue is stiffer would be changed at different stretch level. In fact, this is possible because that the stiffness of the aneurysmal tissues increases faster than normal tissues [21]. This theory probably could also be applied to the case of aortic dissection given our data and previous work showed that the stress-stretch curve of the dissected aortic tissue typically starts lower but goes up more rapidly, compared to normal tissues [22]. Two prior experimental studies on aortic dissection stated that dissected tissues were generally stiffer than normal tissues, especially at high strain conditions [22,52]. But no statistical conclusion can be drawn due to the small sample size in these studies because one study had none normal aortic specimen [52] while the other only had one dissected

specimen [22]. Based on 18 subjects, our statistical analysis in layer-specific mechanical properties between diseased and normal aortic tissues showed that diseased IM samples was significantly stiffer than normal IM samples in longitudinal direction at stretch ratio 1.3, but not in circumferential direction (see Fig. 4). This suggests that the IM layer has been subjected to significant mechanical properties change during the pathological development of aortic dissection. Amabili et al. also claimed some mechanical anomalies of the media and adventitia were associated with aortic dissection [22]. However, our data does not support the mechanical anomaly in the adventitia layer. To best of our knowledge, this is the first report on the comparison analysis between normal and dissected aortic tissues in a layer-specific manner with enough statistical power.

4.2. Effects of aortic tissue histology on mechanical properties

Elastic and collagen fibers are important loading-bearing aortic tissue compositions in the aortic wall [44]. Change in mechanical properties of aortic wall was fundamentally rooted in the tissue remodeling as these aortic tissue compositions undergo dynamic synthesis and degradation, and crosslinking [11,53]. By comparing two tissue groups, the elastic fiber densities in IW and IM samples from diseased group were smaller than those from normal group. This is consistent with previous histopathological findings that aortic dissection was associated with medial degeneration characterized by elastic fiber fragmentation and loss [54,55]. However, our results showed that the difference is not statistically significant, probably due to the small sample size in the present study.

As the most important contributor to the elastic properties of the aorta, elastic fiber content decreased in diseased aortic tissue make it less capable to resist the external loading at low stretch level [56]. Therefore, a small load would considerably elongate the diseased aorta, leading to a small tissue stiffness at low stretch level, which is consistent with our data. It is also reported that elastin serves an important role in stabilizing the aortic structure, and decreased elastin content was considered as the predisposing factor for aortic dissection [4,56], which was later experimentally confirmed by an animal study [57].

Compared to elastic fiber, collagen fiber is much stiffer when straightened at physiological stretch level [56]. The higher collagen fiber density in diseased tissue samples means that large forces were required to stretch the aortic tissue at high stretch level [56]. This might explain why the material stiffness of diseased tissue samples increased faster than that of normal tissue samples when stretch level increased (see Fig. 3 and Table 3). Nevertheless, it should be noted that the fiber density is not the only factor contributing to the aortic mechanical properties, the cross-linking between these fibers and other components like glycosaminoglycans, proteoglycans and matrix Metalloproteinases also are prominent contributions to the aortic mechanical properties [20,58].

4.3. Implication for dissection risk assessment

The significant difference in mechanical properties of IM samples between diseased and normal groups at stretch level 1.3 indicated that, during the aortic dissection process, the intima-media layer was more influenced by the disease process. Together with noticeable decrease in elastic fiber density in this layer, it is evidently showed that the mechanical and microstructural alternations occurred in the intima-media layer during the pathological process, which may be associated with occurrence of aortic dissection [4,55]. Compared to IM layer, the adventitia layer was less affected by the disease as it underwent relatively smaller mechanical and compositional alternations. This coincides with the clinical observation that the intimal tear normally progresses into the aortic media, but not into adventitia layer [5]. All these evidence points to the fact that IM sample stiffness may be used as an indicator for aortic dissection risk assessment in the future, especially when it is possible to measure the stiffness of the intima-media layer in clinical setting. In fact, there are some methods proposed to estimate the material properties/stiffness of the aortic wall in vivo using clinical data including medical images of aortic wall, pulsatile pressure conditions and other information [59,60]. However, in these methods, the aortic wall was treated as a homogenous material, not a heterogeneous material with different tissue layers due to some limitations such as low resolution of imaging techniques to differentiate aortic layer, the accuracy of pressure measurements. With the advance of imaging and measurement techniques to obtain more accurate clinical information, it would come true to accurately and efficiently quantify the layer-specific material properties of aortic wall in clinical setting [59,60].

4.4. Limitations

(1) Histology. The quantitative measurements of elastic and collagen fiber densities depend on subsample selection for histological staining [37]. Besides, in order to perform both the mechanical and histological characterizations, the samples were histologically examined after the biaxial tensile testing. Although tensile testing does not affect the composition of aortic tissue, it could influence the tissue architectures, such as loose collagen fibers in adventitia and separation of some smooth muscle cells in media [31]; Care was taken to select the subsample least influenced by the tensile testing for histological staining. (2) Shear strain/stress terms were not considered in the current study. Previous studies have shown that the shear strain/stress was significant smaller, compared to the normal strain/stress in the biaxial tensile testing [32]. Therefore, it is reasonable to treat them as zeros when performing the constitutive modeling of the aortic tissues; (3) Only the elastic and collagen fibers were analyzed in this study. Other tissue constituents such as the cytoplasm, glycosaminoglycans, and matrix Metalloproteinases which also influence the mechanical behavior of the aortic tissue were not considered [46], and will be included in future investigation when data become available. (4) Sample size. The sample size is small in our study. Large-scale patient studies are needed for further validation.

5. Conclusion

Compared to normal aortic tissues, the elastic fiber density of the intima-media layer in the dissected aortic tissue was lower, while its tissue stiffness was significantly higher in the dissected aortic tissues, indicating the tissue stiffness of the intima-media layer could be a potential indicator for aortic dissection risk assessment.

Data availability statement

The data that support the findings of this study are available on request from the corresponding author, and the data associated with this study have not been deposited in a publicly available repository.

Ethics declarations

This study was reviewed and approved by Medical Ethics Committee of Jiangsu Province Hospital with the approval number: 2022-SR-730, dated December 30, 2022. All participants/patients or their proxies provided written informed consent for the publication of their anonymized case details and images.

CRediT authorship contribution statement

Xiaoya Guo: Writing – review & editing, Writing – original draft, Visualization, Methodology, Funding acquisition, Formal analysis. **Han Yu:** Writing – review & editing, Investigation. **Liang Wang:** Writing – review & editing, Writing – original draft, Supervision, Methodology, Conceptualization. **Yali Zhai:** Writing – review & editing, Investigation. **Jiantao Li:** Writing – review & editing, Investigation, Conceptualization. **Dalin Tang:** Writing – review & editing. **Haoliang Sun:** Writing – review & editing, Resources, Funding acquisition, Conceptualization.

Declaration of competing interest

The authors declare that they have no known competing financial interests or personal relationships that could have appeared to influence the work reported in this paper.

Acknowledgments

This research was supported by National Natural Sciences Foundation of China [82100254] and the Foundation of Jiangsu Provincial Double-Innovation Doctor Program [CZ007SC20006].

Appendix A. Supplementary data

Supplementary data to this article can be found online at https://doi.org/10.1016/j.heliyon.2024.e34646.

References

[1] P.G. Hagan, C.A. Nienaber, E.M. Isselbacher, D. Bruckman, D.J. Karavite, P.L. Russman, A. Evangelista, R. Fattori, T. Suzuki, J.K. Oh, A.G. Moore, J.F. Malouf, L. A. Pape, C. Gaca, U. Sechtem, S. Lenferink, H.J. Deutsch, H. Diedrichs, J.M.Y. Robles, A. Llovet, D. Gilon, S.K. Das, W.F. Armstrong, G.M. Deeb, K.A. Eagle, The International Registry of acute aortic dissection (IRAD) - new insights into an old disease, JAMA, J. Am. Med. Assoc. 283 (7) (2000) 897–903.
[2] A. Evangelista, E.M. Isselbacher, E. Bossone, T.G. Gleason, M. Di Eusanio, U. Sechtem, M.P. Ehrlich, S. Trimarchi, A.C. Braverman, T. Myrmel, K.M. Harris, S. Hutchinson, P. O'Gara, T. Suzuki, C.A. Nienaber, K.A. Eagle, I. Investigators, Insights from the International Registry of acute aortic dissection A 20-Year experience of Collaborative clinical research, Circulation 137 (17) (2018) 1846–1860.
[3] S.A. LeMaire, L. Russell, Epidemiology of thoracic aortic dissection, Nat. Rev. Cardiol. 8 (2) (2011) 103–113.
[4] M.A. Cattell, P.S. Hasleton, J.C. Anderson, Increased elastin content and decreased elastin concentration may be predisposing factors in dissecting aneurysms of human thoracic aorta, Cardiovasc. Res. 27 (2) (1993) 176–181.
[5] H. Ogino, O. Iida, K. Akutsu, Y. Chiba, H. Hayashi, H. Ishibashi-Ueda, S. Kaji, M. Kato, K. Komori, H. Matsuda, K. Minatoya, H. Morisaki, T. Ohki, Y. Saiki, K. Shigematsu, N. Shiiya, H. Shimizu, N. Azuma, H. Higami, S. Ichihashi, T. Iwahashi, K. Kamiya, T. Katsumata, N. Kawaharada, Y. Kinoshita, T. Matsumoto, S. Miyamoto, T. Morisaki, T. Morota, K. Nanto, T. Nishibe, K. Okada, K. Orihashi, J. Tazaki, M. Toma, T. Tsukube, K. Uchida, T. Ueda, A. Usui, K. Yamanaka, H. Yamauchi, K. Yoshioka, T. Kimura, T. Miyata, Y. Okita, M. Ono, Y. Ueda, JCS/JSCVS/JATS/JSVS 2020 Guideline on Diagnosis and Treatment of aortic aneurysm and aortic dissection, Circ. J. 87 (10) (2023) 1410–1621.
[6] E.M. Isselbacher, O. Preventza, J.H. Black, J.G. Augoustides, A.W. Beck, M.A. Bolen, A.C. Braverman, B.E. Bray, M.M. Brown-Zimmerman, E.P. Chen, T. J. Collins, A. DeAnda, C.L. Fanola, L.N. Girardi, C.W. Hicks, D.S. Hui, W.S. Jones, V. Kalahasti, K.M. Kim, D.M. Milewicz, G.S. Oderich, L. Ogbechie, S.B. Promes, E.G. Ross, M.L. Schermerhorn, S.S. Times, E.E. Tseng, G.J. Wang, Y.J. Woo, C. Writing, ACC/AHA Guideline for the Diagnosis and Management of aortic disease: a report of the American Heart association/American College of Cardiology Joint Committee on clinical Practice Guidelines, Circulation 146 (24) (2022) E334–E482. \.
[7] J.D. Humphrey, E.R. Dufresne, M.A. Schwartz, Mechanotransduction and extracellular matrix homeostasis, Nat. Rev. Mol. Cell Biol. 15 (12) (2014) 802–812.
[8] S. Sherifova, G.A. Holzapfel, Biomechanics of aortic wall failure with a focus on dissection and aneurysm: a review, Acta Biomater. 99 (2019) 1–17.
[9] N. Choudhury, O. Bouchot, L. Rouleau, D. Tremblay, R. Cartier, J. Butany, R. Mongrain, R.L. Leask, Local mechanical and structural properties of healthy and diseased human ascending aorta tissue, Cardiovasc. Pathol. 18 (2) (2009) 83–91.

[10] J. Brunet, B. Pierrat, P. Badel, Review of current advances in the mechanical Description and Quantification of aortic dissection mechanisms, Ieee Reviews in Biomedical Engineering 14 (2021) 240–255.
[11] K. Linka, C. Cavinato, J.D. Humphrey, C.J. Cyron, Predicting and understanding arterial elasticity from key microstructural features by bidirectional deep learning, Acta Biomater. 147 (2022) 63–72.
[12] A. Tsamis, J.T. Krawiec, D.A. Vorp, Elastin and collagen fibre microstructure of the human aorta in ageing and disease: a review, Journal of the Royal Society Interface 10 (83) (2013).
[13] D.P. Sokolis, E.P. Kritharis, A.T. Giagini, K.M. Lampropoulos, S.A. Papadodima, D.C. Iliopoulos, Biomechanical response of ascending thoracic aortic aneurysms: association with structural remodelling, Comput. Methods Biomech. Biomed. Eng. 15 (3) (2012) 231–248.
[14] Z.F. Li, T. Luo, S. Wang, H.Y. Jia, Q. Gong, X.P. Liu, M.P. Sutcliffe, H.J. Zhu, Q. Liu, D.D. Chen, J. Xiong, Z.Z. Teng, Mechanical and histological characteristics of aortic dissection tissues, Acta Biomater. 146 (2022) 284–294.
[15] S.K. Bhat, H. Yamada, Mechanical characterization of dissected and dilated human ascending aorta using Fung-type hyperelastic models with pre-identified initial tangent moduli for low-stress distensibility, J. Mech. Behav. Biomed. Mater. 125 (2022).
[16] LdF. Borges, R.G. Jaldin, R.R. Dias, N.A. Groppo Stolf, J.-B. Michel, P.S. Gutierrez, Collagen is reduced and disrupted in human aneurysms and dissections of ascending aorta, Hum. Pathol. 39 (3) (2008) 437–443.
[17] O. Leone, D. Pacini, A. Foà, A. Corsini, V. Agostini, B. Corti, L. Di Marco, A. Leone, M. Lorenzini, L.B. Reggiani, R. Di Bartolomeo, C. Rapezzi, Redefining the histopathologic profile of acute aortic syndromes: clinical and prognostic implications, J. Thorac. Cardiovasc. Surg. 156 (5) (2018) 1776–1785.
[18] A. Pukaluk, H. Wolinski, C. Viertler, P. Regitnig, G.A. Holzapfel, G. Sommer, Changes in the microstructure of the human aortic medial layer under biaxial loading investigated by multi-photon microscopy, Acta Biomater. 151 (2022) 396–413.
[19] A. Pukaluk, H. Wolinski, C. Viertler, P. Regitnig, G.A. Holzapfel, G. Sommer, Changes in the microstructure of the human aortic adventitia under biaxial loading investigated by multi-photon microscopy, Acta Biomater. 161 (2023) 154–169.
[20] X.C. Wang, H.J. Carpenter, M.H. Ghayesh, A. Kotousov, A.C. Zander, M. Amabili, P.J. Psaltis, A review on the biomechanical behaviour of the aorta, J. Mech. Behav. Biomed. Mater. 144 (2023).
[21] M. Nightingale, A. Gregory, T. Sigaeva, G.M. Dobson, P.W.M. Fedak, J.J. Appoo, E.S. Di Martino, University of Calgary Aorta At-Risk Working G, Biomechanics in ascending aortic aneurysms correlate with tissue composition and strength, JTCVS open 9 (2022) 1–10.
[22] M. Amabili, G.O. Arena, P. Balasubramanian, I.D. Breslavsky, R. Cartier, G. Ferrari, G.A. Holzapfel, A. Kassab, R. Mongrain, Biomechanical characterization of a chronic type a dissected human aorta, J. Biomech. 110 (2020).
[23] V. Deplano, M. Boufi, V. Gariboldi, A.D. Loundou, X.B. D'Journo, J. Cautela, A. Djemli, Y.S. Alimi, Mechanical characterisation of human ascending aorta dissection, J. Biomech. 94 (2019) 138–146.
[24] M. Amabili, M. Asgari, I.D. Breslavsky, G. Franchini, F. Giovanniello, G.A. Holzapfel, Microstructural and mechanical characterization of the layers of human descending thoracic aortas, Acta Biomater. 134 (2021) 401–421.
[25] W.G. Ma, J.M. Zhu, J. Zheng, Y.M. Liu, B.A. Ziganshin, J.A. Elefteriades, L.Z. Sun, Sun's procedure for complex aortic arch repair: total arch replacement using a tetrafurcate graft with stented elephant trunk implantation, Ann. Cardiothorac. Surg. 2 (5) (2013) 642–648.
[26] C. Martin, T. Pham, W. Sun, Significant differences in the material properties between aged human and porcine aortic tissues, Eur. J. Cardio. Thorac. Surg. 40 (1) (2011) 28–34.
[27] M.H. Kural, M. Cai, D. Tang, T. Gwyther, J. Zheng, K.L. Billiar, Planar biaxial characterization of diseased human coronary and carotid arteries for computational modeling, J. Biomech. 45 (5) (2012) 790–798.
[28] M. Amabili, P. Balasubramanian, I. Bozzo, I.D. Breslaysky, G. Ferrari, Layer-specific hyperelastic and viscoelastic characterization of human descending thoracic aortas, J. Mech. Behav. Biomed. Mater. 99 (2019) 27–46.
[29] Q. Lin, S. Shi, L. Wang, S. Chen, X. Chen, G. Chen, In-plane biaxial cyclic mechanical behavior of proton exchange membranes, J. Power Sources 360 (2017) 495–503.
[30] X. Guo, C. Gong, Y. Zhai, H. Yu, J. Li, H. Sun, L. Wang, D. Tang, Biomechanical characterization of normal and pathological human ascending aortic tissues via biaxial testing Experiment, constitutive modeling and finite element analysis, Comput. Biol. Med. 166 (2023) 107561.
[31] G.A. Holzapfel, G. Sommer, C.T. Gasser, P. Regitnig, Determination of layer-specific mechanical properties of human coronary arteries with nonatherosclerotic intimal thickening and related constitutive modeling, Am. J. Physiol. Heart Circ. Physiol. 289 (5) (2005) H2048–H2058.
[32] J.A. Pena, M.A. Martinez, E. Pena, Layer-specific residual deformations and uniaxial and biaxial mechanical properties of thoracic porcine aorta, J. Mech. Behav. Biomed. Mater. 50 (2015) 55–69.
[33] J. Takada, K. Hamada, X. Zhu, Y. Tsuboko, K. Iwasaki, Biaxial tensile testing system for measuring mechanical properties of both sides of biological tissues, J. Mech. Behav. Biomed. Mater. 146 (2023).
[34] V. Deplano, M. Boufi, O. Boiron, C. Guivier-Curien, Y. Alimi, E. Bertrand, Biaxial tensile tests of the porcine ascending aorta, J. Biomech. 49 (10) (2016) 2031–2037.
[35] J.A. Niestrawska, C. Viertler, P. Regitnig, T.U. Cohnert, G. Sommer, G.A. Holzapfel, Microstructure and mechanics of healthy and aneurysmatic abdominal aortas: experimental analysis and modelling, Journal of the Royal Society Interface 13 (124) (2016).
[36] Y.H. Chim, H.A. Davies, D. Mason, O. Nawaytou, M. Field, J. Madine, R. Akhtar, Bicuspid valve aortopathy is associated with distinct patterns of matrix degradation, J. Thorac. Cardiovasc. Surg. 160 (6) (2020) E239–E257.
[37] T.L. Surman, J.M. Abrahams, J. Manavis, J. Finnie, D. O'Rourke, K.J. Reynolds, J. Edwards, M.G. Worthington, J. Beltrame, Histological regional analysis of the aortic root and thoracic ascending aorta: a complete analysis of aneurysms from root to arch, J. Cardiothorac. Surg. 16 (1) (2021).
[38] S.S. Shapiro, M.B. Wilk, An analysis of variance test for normality (complete samples), Biometrika 52 (3/4) (1965) 591–611.
[39] H.B. Mann, D.R. Whitney, On a test of whether one of two random variables is stochastically larger than the other, Ann. Math. Stat. (1947) 50–60.
[40] Z. Teng, Y. Zhang, Y. Huang, J. Feng, J. Yuan, Q. Lu, M.P. Sutcliffe, A.J. Brown, Z. Jing, J.H. Gillard, Material properties of components in human carotid atherosclerotic plaques: a uniaxial extension study, Acta Biomater. 10 (12) (2014) 5055–5063.
[41] M.R. Labrosse, C.J. Beller, T. Mesana, J.P. Veinot, Mechanical behavior of human aortas: Experiments, material constants and 3-D finite element modeling including residual stress, J. Biomech. 42 (8) (2009) 996–1004.
[42] Z.Q. Yin, H. Han, X.C. Yan, Q.J. Zheng, Research progress on the Pathogenesis of aortic dissection, Curr. Probl. Cardiol. 48 (8) (2023).
[43] J.D. Humphrey, M.A. Schwartz, Vascular Mechanobiology: homeostasis, Adaptation, and disease, Annu. Rev. Biomed. Eng. 23 (1) (2021) 1–27.
[44] J.D. Humphrey, D.M. Milewicz, G. Tellides, M.A. Schwartz, Dysfunctional Mechanosensing in aneurysms, Science 344 (6183) (2014) 476–478.
[45] G.A. Holzapfel, T.C. Gasser, R.W. Ogden, A new constitutive framework for arterial wall mechanics and a comparative study of material models, Journal of elasticity and the physical science of solids 61 (2000) 1–48.
[46] D. Weiss, B.V. Rego, C. Cavinato, D.S. Li, Y. Kawamura, N. Emuna, J.D. Humphrey, Effects of age, sex, and extracellular matrix integrity on aortic dilatation and rupture in a mouse model of Marfan syndrome, Arterioscler. Thromb. Vasc. Biol. 43 (9) (2023) e358–e372.
[47] M. Jadidi, S. Sherifova, G. Sommer, A. Kamenskiy, G.A. Holzapfel, Constitutive modeling using structural information on collagen fiber direction and dispersion in human superficial femoral artery specimens of different ages, Acta Biomater. 121 (2021) 461–474.
[48] D.A. Vorp, B.J. Schiro, M.P. Ehrlich, T.S. Juvonen, M.A. Ergin, B.P. Griffith, Effect of aneurysm on the tensile strength and biomechanical behavior of the ascending thoracic aorta, Ann. Thorac. Surg. 75 (4) (2003) 1210–1214.
[49] A.N. Azadani, S. Chitsaz, A. Mannion, A. Mookhoek, A. Wisneski, J.M. Guccione, M.D. Hope, L. Ge, E.E. Tseng, Biomechanical properties of human ascending thoracic aortic aneurysms, Ann. Thorac. Surg. 96 (1) (2013) 50–58.
[50] G. Koullias, R. Modak, M. Tranquilli, D.P. Korkolis, P. Barash, J.A. Elefteriades, Mechanical deterioration underlies malignant behavior of aneurysmal human ascending aorta, J. Thorac. Cardiovasc. Surg. 130 (3) (2005) 677–683.
[51] R.J. Okamoto, H.D. Xu, N.T. Kouchoukos, M.R. Moon, T.M. Sundt, The influence of mechanical properties on wall stress and distensibility of the dilated ascending aorta, J. Thorac. Cardiovasc. Surg. 126 (3) (2003) 842–850.

[52] A.R. Babu, A.G. Byju, N. Gundiah, Biomechanical properties of human ascending thoracic aortic dissections, Journal of Biomechanical Engineering-Transactions of the Asme 137 (8) (2015).
[53] D. Wagsater, V. Paloschi, R. Hanemaaijer, K. Hultenby, R.A. Bank, A. Franco-Cereceda, J.H.N. Lindeman, P. Eriksson, Impaired collagen Biosynthesis and cross-linking in aorta of patients with Bicuspid aortic valve, J. Am. Heart Assoc. 2 (1) (2013).
[54] H. Sariola, T. Viljanen, R. Luosto, Histological pattern and changes in extracellular-matrix in aortic dissections, J. Clin. Pathol. 39 (10) (1986) 1074–1081.
[55] M.K. Halushka, A. Angelini, G. Bartoloni, C. Basso, L. Batoroeva, P. Bruneval, L.M. Buja, J. Butany, G. d'Amati, J.T. Fallon, P.J. Gallagher, A.C. Gittenberger-de Groot, R.H. Gouveia, I. Kholova, K.L. Kelly, O. Leone, S.H. Litovsky, J.J. Maleszewski, D.V. Miller, R.N. Mitchell, S.D. Preston, A. Pucci, S.J. Radio, E. R. Rodriguez, M.N. Sheppard, J.R. Stone, S.K. Suvarna, C.D. Tan, G. Thiene, J.P. Veinot, A.C. van der Wal, Consensus statement on surgical pathology of the aorta from the Society for Cardiovascular Pathology and the Association for European Cardiovascular Pathology: II. Noninflammatory degenerative diseases - nomenclature and diagnostic criteria, Cardiovasc. Pathol. 25 (3) (2016) 247–257.
[56] M.R. Roach, A.C. Burton, The reason for the shape of the distensibility curves of arteries, Can. J. Biochem. Physiol. 35 (8) (1957) 681–690.
[57] C.L. Crandall, B. Caballero, M.E. Viso, N.R. Vyavahare, J.E. Wagenseil, Pentagalloyl Glucose (PGG) prevents and Restores mechanical changes caused by elastic fiber fragmentation in the mouse ascending aorta, Ann. Biomed. Eng. 51 (4) (2023) 806–819.
[58] S. Roccabianca, G.A. Ateshian, J.D. Humphrey, Biomechanical roles of medial pooling of glycosaminoglycans in thoracic aortic dissection, Biomech. Model. Mechanobiol. 13 (1) (2014) 13–25.
[59] M. Liu, L. Liang, W. Sun, A new inverse method for estimation of in vivo mechanical properties of the aortic wall, Journal of the mechanical behavior of biomedical materials 72 (2017) 148–158.
[60] S. Laurent, J. Cockcroft, L. Van Bortel, P. Boutouyrie, C. Giannattasio, D. Hayoz, B. Pannier, C. Vlachopoulos, I. Wilkinson, H. Struijker-Boudier, N-i European Network, Expert consensus document on arterial stiffness: methodological issues and clinical applications, Eur. Heart J. 27 (21) (2006) 2588–2605.